

Search for New Physics Using High Mass Tau Pairs from 1.96-TeV $p\bar{p}$ Collisions

D. Acosta,¹⁶ J. Adelman,¹² T. Affolder,⁹ T. Akimoto,⁵⁴ M.G. Albrow,¹⁵ D. Ambrose,¹⁵ S. Amerio,⁴² D. Amidei,³³ A. Anastassov,⁵⁰ K. Anikeev,¹⁵ A. Annovi,⁴⁴ J. Antos,¹ M. Aoki,⁵⁴ G. Apollinari,¹⁵ T. Arisawa,⁵⁶ J-F. Arguin,³² A. Artikov,¹³ W. Ashmanskas,¹⁵ A. Attal,⁷ F. Azfar,⁴¹ P. Azzi-Bacchetta,⁴² N. Bacchetta,⁴² H. Bachacou,²⁸ W. Badgett,¹⁵ A. Barbaro-Galtieri,²⁸ G.J. Barker,²⁵ V.E. Barnes,⁴⁶ B.A. Barnett,²⁴ S. Baroiant,⁶ G. Bauer,³¹ F. Bedeschi,⁴⁴ S. Behari,²⁴ S. Belforte,⁵³ G. Bellettini,⁴⁴ J. Bellinger,⁵⁸ A. Belloni,³¹ E. Ben-Haim,¹⁵ D. Benjamin,¹⁴ A. Beretvas,¹⁵ T. Berry,²⁹ A. Bhatti,⁴⁸ M. Binkley,¹⁵ D. Bisello,⁴² M. Bishai,¹⁵ R.E. Blair,² C. Blocker,⁵ K. Bloom,³³ B. Blumenfeld,²⁴ A. Bocci,⁴⁸ A. Bodek,⁴⁷ G. Bolla,⁴⁶ A. Bolshov,³¹ D. Bortoletto,⁴⁶ J. Boudreau,⁴⁵ S. Bourov,¹⁵ B. Brau,⁹ C. Bromberg,³⁴ E. Brubaker,¹² J. Budagov,¹³ H.S. Budd,⁴⁷ K. Burkett,¹⁵ G. Busetto,⁴² P. Bussey,¹⁹ K.L. Byrum,² S. Cabrera,¹⁴ M. Campanelli,¹⁸ M. Campbell,³³ F. Canelli,⁷ A. Canepa,⁴⁶ M. Casarsa,⁵³ D. Carlsmith,⁵⁸ R. Carosi,⁴⁴ S. Carron,¹⁴ M. Cavalli-Sforza,³ A. Castro,⁴ P. Catastini,⁴⁴ D. Cauz,⁵³ A. Cerri,²⁸ L. Cerrito,⁴¹ J. Chapman,³³ Y.C. Chen,¹ M. Chertok,⁶ G. Chiarelli,⁴⁴ G. Chlachidze,¹³ F. Chlebana,¹⁵ I. Cho,²⁷ K. Cho,²⁷ D. Chokheli,¹³ J.P. Chou,²⁰ S. Chuang,⁵⁸ K. Chung,¹¹ W-H. Chung,⁵⁸ Y.S. Chung,⁴⁷ M. Cijliak,⁴⁴ C.I. Ciobanu,²³ M.A. Ciocci,⁴⁴ A.G. Clark,¹⁸ D. Clark,⁵ M. Coca,¹⁴ A. Connolly,²⁸ M. Convery,⁴⁸ J. Conway,⁶ B. Cooper,³⁰ K. Copic,³³ M. Cordelli,¹⁷ G. Cortiana,⁴² J. Cranshaw,⁵² J. Cuevas,¹⁰ A. Cruz,¹⁶ R. Culbertson,¹⁵ C. Currat,²⁸ D. Cyr,⁵⁸ D. Dagenhart,⁵ S. Da Ronco,⁴² S. D'Auria,¹⁹ P. de Barbaro,⁴⁷ S. De Cecco,⁴⁹ A. Deisher,²⁸ G. De Lentdecker,⁴⁷ M. Dell'Orso,⁴⁴ S. Demers,⁴⁷ L. Demortier,⁴⁸ M. Deninno,⁴ D. De Pedis,⁴⁹ P.F. Derwent,¹⁵ T. Devlin,⁵⁰ C. Dionisi,⁴⁹ J.R. Dittmann,¹⁵ P. DiTuro,⁵⁰ C. Dörr,²⁵ A. Dominguez,²⁸ S. Donati,⁴⁴ M. Donega,¹⁸ J. Donini,⁴² M. D'Onofrio,¹⁸ T. Dorigo,⁴² K. Ebina,⁵⁶ J. Efron,³⁸ J. Ehlers,¹⁸ R. Erbacher,⁶ M. Erdmann,²⁵ D. Errede,²³ S. Errede,²³ R. Eusebi,⁴⁷ H-C. Fang,²⁸ S. Farrington,²⁹ I. Fedorko,⁴⁴ W.T. Fedorko,¹² R.G. Feild,⁵⁹ M. Feindt,²⁵ J.P. Fernandez,⁴⁶ R.D. Field,¹⁶ G. Flanagan,³⁴ L.R. Flores-Castillo,⁴⁵ A. Foland,²⁰ S. Forrester,⁶ G.W. Foster,¹⁵ M. Franklin,²⁰ J.C. Freeman,²⁸ Y. Fujii,²⁶ I. Furic,¹² A. Gajjar,²⁹ M. Gallinaro,⁴⁸ J. Galyardt,¹¹ M. Garcia-Sciveres,²⁸ A.F. Garfinkel,⁴⁶ C. Gay,⁵⁹ H. Gerberich,¹⁴ D.W. Gerdes,³³ E. Gerchtein,¹¹ S. Giagu,⁴⁹ P. Giannetti,⁴⁴ A. Gibson,²⁸ K. Gibson,¹¹ C. Ginsburg,¹⁵ K. Giolo,⁴⁶ M. Giordani,⁵³ M. Giunta,⁴⁴ G. Giurgiu,¹¹ V. Glagolev,¹³ D. Glenzinski,¹⁵ M. Gold,³⁶ N. Goldschmidt,³³ D. Goldstein,⁷ J. Goldstein,⁴¹ G. Gomez,¹⁰ G. Gomez-Ceballos,¹⁰ M. Goncharov,⁵¹ O. González,⁴⁶ I. Gorelov,³⁶ A.T. Goshaw,¹⁴ Y. Gotra,⁴⁵ K. Goulianos,⁴⁸ A. Gresele,⁴² M. Griffiths,²⁹ C. Grosso-Pilcher,¹² U. Grundler,²³ J. Guimaraes da Costa,²⁰ C. Haber,²⁸ K. Hahn,⁴³ S.R. Hahn,¹⁵ E. Halkiadakis,⁴⁷ A. Hamilton,³² B-Y. Han,⁴⁷ R. Handler,⁵⁸ F. Happacher,¹⁷ K. Hara,⁵⁴ M. Hare,⁵⁵ R.F. Harr,⁵⁷ R.M. Harris,¹⁵ F. Hartmann,²⁵ K. Hatakeyama,⁴⁸ J. Hauser,⁷ C. Hays,¹⁴ H. Hayward,²⁹ B. Heinemann,²⁹ J. Heinrich,⁴³ M. Hennecke,²⁵ M. Herndon,²⁴ C. Hill,⁹ D. Hirschbuehl,²⁵ A. Hocker,¹⁵ K.D. Hoffman,¹² A. Holloway,²⁰ S. Hou,¹ M.A. Houlden,²⁹ B.T. Huffman,⁴¹ Y. Huang,¹⁴ R.E. Hughes,³⁸ J. Huston,³⁴ K. Ikado,⁵⁶ J. Incandela,⁹ G. Introzzi,⁴⁴ M. Iori,⁴⁹ Y. Ishizawa,⁵⁴ C. Issever,⁹ A. Ivanov,⁶ Y. Iwata,²² B. Iyutin,³¹ E. James,¹⁵ D. Jang,⁵⁰ B. Jayatilaka,³³ D. Jeans,⁴⁹ H. Jensen,¹⁵ E.J. Jeon,²⁷ M. Jones,⁴⁶ K.K. Joo,²⁷ S.Y. Jun,¹¹ T. Junk,²³ T. Kamon,⁵¹ J. Kang,³³ M. Karagoz Unel,³⁷ P.E. Karchin,⁵⁷ Y. Kato,⁴⁰ Y. Kemp,²⁵ R. Kephart,¹⁵ U. Kerzel,²⁵ V. Khotilovich,⁵¹ B. Kilminster,³⁸ D.H. Kim,²⁷ H.S. Kim,²³ J.E. Kim,²⁷ M.J. Kim,¹¹ M.S. Kim,²⁷ S.B. Kim,²⁷ S.H. Kim,⁵⁴ Y.K. Kim,¹² M. Kirby,¹⁴ L. Kirsch,⁵ S. Klimenko,¹⁶ M. Klute,³¹ B. Knuteson,³¹ B.R. Ko,¹⁴ H. Kobayashi,⁵⁴ D.J. Kong,²⁷ K. Kondo,⁵⁶ J. Konigsberg,¹⁶ K. Kordas,³² A. Korn,³¹ A. Korytov,¹⁶ A.V. Kotwal,¹⁴ A. Kovalev,⁴³ J. Kraus,²³ I. Kravchenko,³¹ A. Kreymer,¹⁵ J. Kroll,⁴³ M. Kruse,¹⁴ V. Krutelyov,⁵¹ S.E. Kuhlmann,² S. Kwang,¹² A.T. Laasanen,⁴⁶ S. Lai,³² S. Lami,^{44,48} S. Lammel,¹⁵ M. Lancaster,³⁰ R. Lander,⁶ K. Lannon,³⁸ A. Lath,⁵⁰ G. Latino,⁴⁴ I. Lazzizzera,⁴² C. Lecci,²⁵ T. LeCompte,² J. Lee,²⁷ J. Lee,⁴⁷ S.W. Lee,⁵¹ R. Lefèvre,³ N. Leonardo,³¹ S. Leone,⁴⁴ S. Levy,¹² J.D. Lewis,¹⁵ K. Li,⁵⁹ C. Lin,⁵⁹ C.S. Lin,¹⁵ M. Lindgren,¹⁵ E. Lipeles,⁸ T.M. Liss,²³ A. Lister,¹⁸ D.O. Litvintsev,¹⁵ T. Liu,¹⁵ Y. Liu,¹⁸ N.S. Lockyer,⁴³ A. Loginov,³⁵ M. Loretì,⁴² P. Loverre,⁴⁹ R-S. Lu,¹ D. Lucchesi,⁴² P. Lujan,²⁸ P. Lukens,¹⁵ G. Lungu,¹⁶ L. Lyons,⁴¹ J. Lys,²⁸ R. Lysak,¹ E. Lytken,⁴⁶ D. MacQueen,³² R. Madrak,¹⁵ K. Maeshima,¹⁵ P. Maksimovic,²⁴ G. Manca,²⁹ F. Margaroli,⁴ R. Marginean,¹⁵ C. Marino,²³ A. Martin,⁵⁹ M. Martin,²⁴ V. Martin,³⁷ M. Martínez,³ T. Maruyama,⁵⁴ H. Matsunaga,⁵⁴ M. Mattson,⁵⁷ P. Mazzanti,⁴ K.S. McFarland,⁴⁷ D. McGivern,³⁰ P.M. McIntyre,⁵¹ P. McNamara,⁵⁰ R. McNulty,²⁹ A. Mehta,²⁹ S. Menzemer,³¹ A. Menzione,⁴⁴ P. Merkel,⁴⁶ C. Mesropian,⁴⁸ A. Messina,⁴⁹ T. Miao,¹⁵ N. Miladinovic,⁵ J. Miles,³¹ L. Miller,²⁰ R. Miller,³⁴ J.S. Miller,³³ C. Mills,⁹ R. Miquel,²⁸ S. Miscetti,¹⁷ G. Mitselmakher,¹⁶ A. Miyamoto,²⁶ N. Moggi,⁴ B. Mohr,⁷ R. Moore,¹⁵ M. Morello,⁴⁴ P.A. Movilla Fernandez,²⁸ J. Muelmenstaedt,²⁸ A. Mukherjee,¹⁵ M. Mulhearn,³¹ T. Muller,²⁵ R. Mumford,²⁴ A. Munar,⁴³ P. Murat,¹⁵ J. Nachtman,¹⁵ S. Nahn,⁵⁹ I. Nakano,³⁹ A. Napier,⁵⁵ R. Naporá,²⁴ D. Naumov,³⁶ V. Necula,¹⁶ J. Nielsen,²⁸ T. Nelson,¹⁵ C. Neu,⁴³ M.S. Neubauer,⁸ T. Nigmanov,⁴⁵ L. Nodulman,² O. Norniella,³ T. Ogawa,⁵⁶ S.H. Oh,¹⁴ Y.D. Oh,²⁷ T. Ohsugi,²² T. Okusawa,⁴⁰ R. Oldeman,²⁹ R. Orava,²¹

W. Orejudos,²⁸ K. Osterberg,²¹ C. Pagliarone,⁴⁴ E. Palencia,¹⁰ R. Paoletti,⁴⁴ V. Papadimitriou,¹⁵
 A.A. Paramonov,¹² S. Pashapour,³² J. Patrick,¹⁵ G. Pauletta,⁵³ M. Paulini,¹¹ C. Paus,³¹ D. Pellett,⁶ A. Penzo,⁵³
 T.J. Phillips,¹⁴ G. Piacentino,⁴⁴ J. Piedra,¹⁰ K.T. Pitts,²³ C. Plager,⁷ L. Pondrom,⁵⁸ G. Pope,⁴⁵ X. Portell,³
 O. Poukhov,¹³ N. Pounder,⁴¹ F. Prakoshyn,¹³ A. Pronko,¹⁶ J. Proudfoot,² F. Ptohos,¹⁷ G. Punzi,⁴⁴
 J. Rademacker,⁴¹ M.A. Rahaman,⁴⁵ A. Rakitine,³¹ S. Rappoccio,²⁰ F. Ratnikov,⁵⁰ H. Ray,³³ B. Reisert,¹⁵
 V. Rekovic,³⁶ P. Renton,⁴¹ M. Rescigno,⁴⁹ F. Rimondi,⁴ K. Rinnert,²⁵ L. Ristori,⁴⁴ W.J. Robertson,¹⁴ A. Robson,¹⁹
 T. Rodrigo,¹⁰ S. Rolli,⁵⁵ R. Roser,¹⁵ R. Rossin,¹⁶ C. Rott,⁴⁶ J. Russ,¹¹ V. Rusu,¹² A. Ruiz,¹⁰ D. Ryan,⁵⁵
 H. Saarikko,²¹ S. Sabik,³² A. Safonov,⁶ R. St. Denis,¹⁹ W.K. Sakumoto,⁴⁷ G. Salamanna,⁴⁹ D. Saltzberg,⁷
 C. Sanchez,³ L. Santi,⁵³ S. Sarkar,⁴⁹ K. Sato,⁵⁴ P. Savard,³² A. Savoy-Navarro,¹⁵ P. Schlabach,¹⁵ E.E. Schmidt,¹⁵
 M.P. Schmidt,⁵⁹ M. Schmitt,³⁷ T. Schwarz,³³ L. Scodellaro,¹⁰ A.L. Scott,⁹ A. Scribano,⁴⁴ F. Scuri,⁴⁴ A. Sedov,⁴⁶
 S. Seidel,³⁶ Y. Seiya,⁴⁰ A. Semenov,¹³ F. Semeria,⁴ L. Sexton-Kennedy,¹⁵ I. Sfiligoi,¹⁷ M.D. Shapiro,²⁸ T. Shears,²⁹
 P.F. Shepard,⁴⁵ D. Sherman,²⁰ M. Shimojima,⁵⁴ M. Shochet,¹² Y. Shon,⁵⁸ I. Shreyber,³⁵ A. Sidoti,⁴⁴ A. Sill,⁵²
 P. Sinervo,³² A. Sisakyan,¹³ J. Sjolin,⁴¹ A. Skiba,²⁵ A.J. Slaughter,¹⁵ K. Sliwa,⁵⁵ D. Smirnov,³⁶ J.R. Smith,⁶
 F.D. Snider,¹⁵ R. Snihur,³² M. Soderberg,³³ A. Soha,⁶ S.V. Somalwar,⁵⁰ J. Spalding,¹⁵ M. Spezziga,⁵² F. Spinella,⁴⁴
 P. Squillacioti,⁴⁴ H. Stadie,²⁵ M. Stanitzki,⁵⁹ B. Stelzer,³² O. Stelzer-Chilton,³² D. Stentz,³⁷ J. Strologas,³⁶
 D. Stuart,⁹ J. S. Suh,²⁷ A. Sukhanov,¹⁶ K. Sumorok,³¹ H. Sun,⁵⁵ T. Suzuki,⁵⁴ A. Taffard,²³ R. Tafirout,³²
 H. Takano,⁵⁴ R. Takashima,³⁹ Y. Takeuchi,⁵⁴ K. Takikawa,⁵⁴ M. Tanaka,² R. Tanaka,³⁹ N. Tanimoto,³⁹
 M. Tecchio,³³ P.K. Teng,¹ K. Terashi,⁴⁸ R.J. Tesarek,¹⁵ S. Tether,³¹ J. Thom,¹⁵ A.S. Thompson,¹⁹ E. Thomson,⁴³
 P. Tipton,⁴⁷ V. Tiwari,¹¹ S. Tkaczyk,¹⁵ D. Toback,⁵¹ K. Tollefson,³⁴ T. Tomura,⁵⁴ D. Tonelli,⁴⁴ M. Tönnemann,³⁴
 S. Torre,⁴⁴ D. Torretta,¹⁵ S. Tourneur,¹⁵ W. Trischuk,³² R. Tsuchiya,⁵⁶ S. Tsuno,³⁹ D. Tsybychev,¹⁶ N. Turini,⁴⁴
 F. Ukegawa,⁵⁴ T. Unverhau,¹⁹ S. Uozumi,⁵⁴ D. Usynin,⁴³ L. Vacavant,²⁸ A. Vaiciulis,⁴⁷ A. Varganov,³³
 S. Vejck III,¹⁵ G. Velez,¹⁵ V. Veszpremi,⁴⁶ G. Veramendi,²³ T. Vickey,²³ R. Vidal,¹⁵ I. Vila,¹⁰ R. Vilar,¹⁰
 I. Vollrath,³² I. Volobouev,²⁸ M. von der Mey,⁷ P. Wagner,⁵¹ R.G. Wagner,² R.L. Wagner,¹⁵ W. Wagner,²⁵
 R. Wallny,⁷ T. Walter,²⁵ Z. Wan,⁵⁰ M.J. Wang,¹ S.M. Wang,¹⁶ A. Warburton,³² B. Ward,¹⁹ S. Waschke,¹⁹
 D. Waters,³⁰ T. Watts,⁵⁰ M. Weber,²⁸ W.C. Wester III,¹⁵ B. Whitehouse,⁵⁵ D. Whiteson,⁴³ A.B. Wicklund,²
 E. Wicklund,¹⁵ H.H. Williams,⁴³ P. Wilson,¹⁵ B.L. Winer,³⁸ P. Wittich,⁴³ S. Wolbers,¹⁵ C. Wolfe,¹² M. Wolter,⁵⁵
 M. Worcester,⁷ S. Worm,⁵⁰ T. Wright,³³ X. Wu,¹⁸ F. Würthwein,⁸ A. Wyatt,³⁰ A. Yagil,¹⁵ T. Yamashita,³⁹
 K. Yamamoto,⁴⁰ J. Yamaoka,⁵⁰ C. Yang,⁵⁹ U.K. Yang,¹² W. Yao,²⁸ G.P. Yeh,¹⁵ J. Yoh,¹⁵ K. Yorita,⁵⁶ T. Yoshida,⁴⁰
 I. Yu,²⁷ S. Yu,⁴³ J.C. Yun,¹⁵ L. Zanello,⁴⁹ A. Zanetti,⁵³ I. Zaw,²⁰ F. Zetti,⁴⁴ J. Zhou,⁵⁰ and S. Zucchelli,⁴¹

(CDF Collaboration)

^{1 1} *Institute of Physics, Academia Sinica, Taipei, Taiwan 11529, Republic of China,*

² *Argonne National Laboratory, Argonne, Illinois 60439,*

³ *Institut de Física d'Altes Energies, Universitat Autònoma de Barcelona, E-08193, Bellaterra (Barcelona), Spain,*

⁴ *Istituto Nazionale di Fisica Nucleare, University of Bologna, I-40127 Bologna, Italy,*

⁵ *Brandeis University, Waltham, Massachusetts 02254,*

⁶ *University of California, Davis, Davis, California 95616,*

⁷ *University of California, Los Angeles, Los Angeles, California 90024,*

⁸ *University of California, San Diego, La Jolla, California 92093,*

⁹ *University of California, Santa Barbara, Santa Barbara, California 93106,*

¹⁰ *Instituto de Física de Cantabria, CSIC-University of Cantabria, 39005 Santander, Spain,*

¹¹ *Carnegie Mellon University, Pittsburgh, PA 15213,*

¹² *Enrico Fermi Institute, University of Chicago, Chicago, Illinois 60637,*

¹³ *Joint Institute for Nuclear Research, RU-141980 Dubna, Russia,*

¹⁴ *Duke University, Durham, North Carolina 27708,*

¹⁵ *Fermi National Accelerator Laboratory, Batavia, Illinois 60510,*

¹⁶ *University of Florida, Gainesville, Florida 32611,*

¹⁷ *Laboratori Nazionali di Frascati, Istituto Nazionale di Fisica Nucleare, I-00044 Frascati, Italy,*

¹⁸ *University of Geneva, CH-1211 Geneva 4, Switzerland,*

¹⁹ *Glasgow University, Glasgow G12 8QQ, United Kingdom,*

²⁰ *Harvard University, Cambridge, Massachusetts 02138,*

²¹ *Division of High Energy Physics, Department of Physics, University of Helsinki and Helsinki Institute of Physics, FIN-00014, Helsinki, Finland,*

²² *Hiroshima University, Higashi-Hiroshima 724, Japan,*

²³ *University of Illinois, Urbana, Illinois 61801,*

²⁴ *The Johns Hopkins University, Baltimore, Maryland 21218,*

²⁵ *Institut für Experimentelle Kernphysik, Universität Karlsruhe, 76128 Karlsruhe, Germany,*

²⁶ *High Energy Accelerator Research Organization (KEK), Tsukuba, Ibaraki 305, Japan,*

²⁷ *Center for High Energy Physics: Kyungpook National University, Taegu 702-701; Seoul National University,*

- Seoul 151-742; and SungKyunKwan University, Suwon 440-746; Korea,
- ²⁸ Ernest Orlando Lawrence Berkeley National Laboratory, Berkeley, California 94720,
- ²⁹ University of Liverpool, Liverpool L69 7ZE, United Kingdom,
- ³⁰ University College London, London WC1E 6BT, United Kingdom,
- ³¹ Massachusetts Institute of Technology, Cambridge, Massachusetts 02139,
- ³² Institute of Particle Physics: McGill University, Montréal, Canada H3A 2T8; and University of Toronto, Toronto, Canada M5S 1A7,
- ³³ University of Michigan, Ann Arbor, Michigan 48109,
- ³⁴ Michigan State University, East Lansing, Michigan 48824,
- ³⁵ Institution for Theoretical and Experimental Physics, ITEP, Moscow 117259, Russia,
- ³⁶ University of New Mexico, Albuquerque, New Mexico 87131,
- ³⁷ Northwestern University, Evanston, Illinois 60208,
- ³⁸ The Ohio State University, Columbus, Ohio 43210,
- ³⁹ Okayama University, Okayama 700-8530, Japan,
- ⁴⁰ Osaka City University, Osaka 588, Japan,
- ⁴¹ University of Oxford, Oxford OX1 3RH, United Kingdom,
- ⁴² University of Padova, Istituto Nazionale di Fisica Nucleare, Sezione di Padova-Trento, I-35131 Padova, Italy,
- ⁴³ University of Pennsylvania, Philadelphia, Pennsylvania 19104,
- ⁴⁴ Istituto Nazionale di Fisica Nucleare Pisa, Universities of Pisa, Siena and Scuola Normale Superiore, I-56127 Pisa, Italy,
- ⁴⁵ University of Pittsburgh, Pittsburgh, Pennsylvania 15260,
- ⁴⁶ Purdue University, West Lafayette, Indiana 47907,
- ⁴⁷ University of Rochester, Rochester, New York 14627,
- ⁴⁸ The Rockefeller University, New York, New York 10021,
- ⁴⁹ Istituto Nazionale di Fisica Nucleare, Sezione di Roma 1, University di Roma "La Sapienza," I-00185 Roma, Italy,
- ⁵⁰ Rutgers University, Piscataway, New Jersey 08855,
- ⁵¹ Texas A&M University, College Station, Texas 77843,
- ⁵² Texas Tech University, Lubbock, Texas 79409,
- ⁵³ Istituto Nazionale di Fisica Nucleare, University of Trieste/ Udine, Italy,
- ⁵⁴ University of Tsukuba, Tsukuba, Ibaraki 305, Japan,
- ⁵⁵ Tufts University, Medford, Massachusetts 02155,
- ⁵⁶ Waseda University, Tokyo 169, Japan,
- ⁵⁷ Wayne State University, Detroit, Michigan 48201,
- ⁵⁸ University of Wisconsin, Madison, Wisconsin 53706,
- ⁵⁹ Yale University, New Haven, Connecticut 06520

(Dated: June 13, 2005)

We present the results of a search for anomalous resonant production of tau lepton pairs with large invariant mass, the first such search using the CDF II Detector in Run II of the Tevatron $p\bar{p}$ collider. Such anomalous production could arise from various new physics processes. In a data sample corresponding to 195 pb^{-1} of integrated luminosity we predict 2.8 ± 0.5 events from Standard Model background processes and observe 4. We use this result to set limits on the production of heavy scalar and vector particles decaying to tau lepton pairs.

PACS numbers: 12.60.Cn, 12.60.Fr, 14.60.Fg, 14.60.St, 14.80.Cp

At the Fermilab Tevatron $p\bar{p}$ collider, a number of non-Standard-Model physics processes can lead to events with high-mass tau lepton pairs in the final state. Examples include the resonant production of Higgs scalars in two-Higgs-doublet models [1] at large $\tan\beta$, the ratio of the vacuum expectation value of the two doublets. Two Higgs doublets are required, for example, in the minimal supersymmetric standard model [2], a favored candidate for extending the Standard Model. The heavy scalar and pseudoscalar Higgs bosons in this theory would decay to tau pairs about 9% of the time. Also, in supersymmetry, if R-parity is not conserved, heavy scalar neutrino production could have tau pair decay modes [3]. If there are heavy Z' bosons, these could also produce high mass

tau pairs in the final state, possibly even with enhanced tau couplings [4]. With the large new data sample from Run II of the Tevatron it is thus of great interest to perform a generic search for high-mass tau pairs.

This Letter presents the results of a search for high-mass tau pairs performed using CDF II, the upgraded Collider Detector at Fermilab (CDF) [5]. In 2002 and 2003 CDF recorded a data sample corresponding to 195 pb^{-1} of integrated luminosity of $p\bar{p}$ collisions at a center of mass energy of 1.96 TeV. This is the first such search with the new high-statistics data sample [6] and new tau identification techniques.

Since the tau lepton decays to lighter leptons (e or μ) about 35% of the time, and to low-multiplicity hadronic

states the rest of the time, this analysis selects events with one identified hadronic tau decay (τ_h) and one other tau decay in the final state. Thus, there are three distinct final states, which we denote $e\tau_h$, $\mu\tau_h$, and $\tau_h\tau_h$. The main background to this search comes from Drell-Yan (DY) $Z/\gamma^* \rightarrow \tau^+\tau^-$ production. Since we seek new particles with mass much larger than that of the Z , we use the observed rate for this background (at smaller tau pair masses) as a control sample, and define the signal region as that where the tau pairs have large visible invariant mass, with missing energy due to the neutrinos from the tau decays.

CDF II is a large general purpose detector with an overall cylindrical geometry surrounding the $p\bar{p}$ interaction region [7]. The three-dimensional trajectories of charged particles produced in $p\bar{p}$ collisions are measured starting at radii of 1.5 cm with multiple layers of silicon microstrip detectors, and are measured at outer radii with an axial/stereo wire drift chamber (COT). The tracking system lies inside a uniform 1.4-T magnetic field produced by a superconducting solenoid, with the field oriented along the beam direction. Outside the solenoid lie the electromagnetic calorimeter and the hadronic calorimeters, which are segmented in pseudorapidity (η) [8] and azimuth in a projective “tower” geometry. A set of strip/wire chambers (CES) located at a depth of six radiation lengths aids in reconstructing photons and electrons from the shower shape. Muons are identified by a system of drift chambers placed outside the calorimeter steel, which acts as an absorber for hadrons. The integrated luminosity of the $p\bar{p}$ collisions is measured to an accuracy of 6% using the Cerenkov Luminosity Counters [9].

The $e\tau_h$ and $\mu\tau_h$ events of interest are recorded using triggers designed to select “lepton plus track” events: those with an e or μ with transverse momentum (p_T) greater than 8 GeV/ c and another charged track with $p_T > 5$ GeV/ c identified by the eXtremely Fast Tracker (XFT) portion of the trigger electronics [10] which reconstructs charged tracks in the COT. The efficiency of this trigger is measured using leptons from Z boson decays, the Υ resonance, and photon conversions [11].

For selecting $\tau_h\tau_h$ events we use a trigger designed to select at least one hadronically decaying tau with $E_T > 20$ GeV accompanied by at least 25 GeV missing energy in the plane transverse to the beam direction (\cancel{E}_T). The tau is identified by matching an XFT track with $p_T > 5$ GeV/ c to a calorimeter cluster. Data used from this trigger come from a sample corresponding to the first 72 pb $^{-1}$ of integrated luminosity recorded; this is less than that of the rest of the data used because of subsequent changes due to rate limitations.

Events selected by the triggers were recorded and processed later to reconstruct charged particle tracks, calorimeter clusters, and to identify electrons, muons, photons, jets, and \cancel{E}_T . Electrons and muons are reconstructed using algorithms described in Ref. [7]. Identification of hadronic decays of taus employs a novel “shrink-

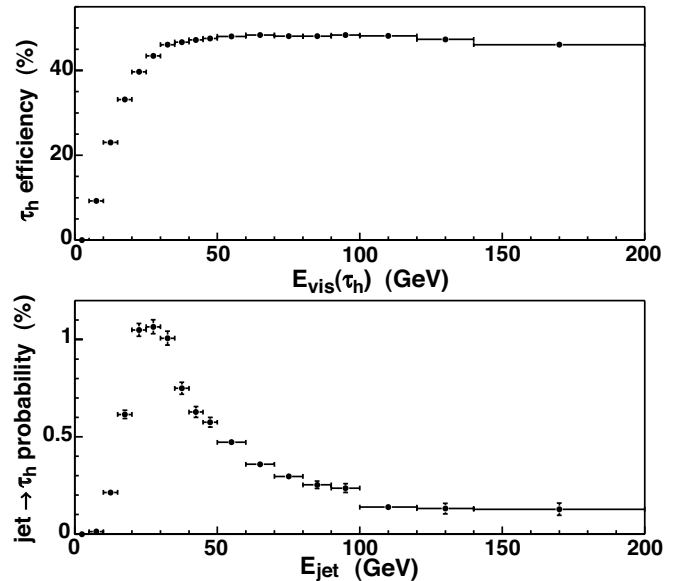


FIG. 1: Identification efficiency (top) and jet $\rightarrow \tau_h$ probability (bottom) as a function of generated tau visible decay product energy and measured jet energy, respectively. The top plot, based on simulation, shows the probability that true hadronically decaying taus are identified as τ_h using the selection in the text. The lower plot shows the probability that hadronic jets in the range $|\eta| < 1$ are misidentified as τ_h , as a function of jet calorimeter cluster energy. The error bars indicate the statistical uncertainties.

ing cone” algorithm based on high- p_T charged tracks in the silicon/COT system, and π^0 candidates identified using the CES by matching strip clusters with wire clusters based on the energy in each.

The τ_h identification algorithm begins with a list of “seed tracks” ranked in p_T , not yet used for another tau candidate, and having $p_T > 6$ GeV/ c . Then it finds the number of other tracks with $p_T > 1$ GeV/ c and π^0 candidates whose momentum vector makes an angle of less than α with the seed track. The angle α is a function of E_{clu} , the energy in the calorimeter cluster associated with the seed track. The value of α is 10° or $(5 \text{ GeV})/E_{clu}$ radians, whichever is less. To allow for resolution effects, the value of α is not less than 100 mrad for π^0 candidates, or 50 mrad for charged tracks. If any other tracks or π^0 candidates have an angle greater than α but less than 30° to the seed track, or if the invariant mass calculated from the sum of all charged track and π^0 candidate four-momenta exceeds 1.8 GeV/ c^2 , the τ_h candidate is rejected. Also, if there is at least 2 GeV of electromagnetic energy in calorimeter towers not part of the tau cluster, and whose centers have $\Delta(R) < 0.4$ from the tau seed track direction, the tau candidate is rejected. Candidates with momentum having an angle of less than 10° with that of a previously identified e or μ are rejected. The algorithm then considers further possible seed tracks, repeating the process until none remain.

The main challenge comes from the large production rate of hadronic jets, which can be misidentified as τ_h . Using the selection described above, Figure 1 shows the efficiency for real hadronically decaying taus with $|\eta| < 1$ to be reconstructed as τ_h , using the simulation discussed below. The figure also shows the jet $\rightarrow \tau_h$ “fake” probability that hadronic jets are misidentified as hadronic tau decays. These jets, reconstructed in a cone size of $\Delta R = \sqrt{(\Delta\eta)^2 + (\Delta\phi)^2} = 0.7$, come from events recorded with triggers requiring various thresholds for calorimeter cluster energy.

To discriminate against background, for the $e\tau_h$ ($\mu\tau_h$) channel the electron (muon) must have a transverse energy of at least 10 GeV, the τ_h must have $E_T > 25$ GeV, and the event must have $\cancel{E}_T > 15$ GeV. For the $\tau_h\tau_h$ channel, one τ_h must have E_T greater than 25 GeV, and the other must have at least 10 GeV. The azimuthal angle between the \cancel{E}_T vector and the e or μ (in $e\tau_h$ or $\mu\tau_h$ events) or the less-energetic of the two in $\tau_h\tau_h$ events must be less than 30° .

For all events selected by the above cuts we calculate the “visible mass” (m_{vis}) by adding the measured four-momenta of the two identified tau decay products in the event to the missing transverse energy four-momentum (for which the z component is taken as zero), and then calculating the invariant mass of the sum. This quantity efficiently distinguishes between lower-mass production of tau pairs (mainly from Z boson decays) and high-mass tau pairs from possible new massive resonant particle production.

The main source of events expected in the selected sample is DY production of Z/γ^* decaying to lepton pair final states, and of these, tau pair production predominates. The production cross section times branching ratio to pairs of each charged lepton species for DY Z/γ^* is assumed to be 250 pb [12] in the mass range 66-116 GeV/ c^2 . For the DY process and for the possible new physics processes discussed below, we simulate the production and decay using the PYTHIA 6.215 Monte Carlo program [13] with CTEQ5L parton distribution functions (PDF’s) [14], with tau decays simulated by TAUOLA [15]. Acceptance and resolution effects come from the full CDF II detector simulation.

The second largest source of events passing our selection criteria is hadronic jets which are misidentified as a τ_h , for example from events with a W boson decaying to a charged lepton and a neutrino plus a jet which passes the τ_h identification criteria. The estimated number of expected events comes from applying the jet $\rightarrow \tau_h$ “fake” rates to jets in events passing the trigger and other requirements, excluding the τ_h identification.

Various systematic uncertainties affect the predicted number of signal and background events. The largest is due to imperfect modeling of the tau identification efficiency. We perform a cross check of this efficiency using $W \rightarrow \tau\nu$ events recorded in the first 72 pb $^{-1}$. Assuming a production cross section times branching ratio to $\tau\nu$ of 2688 pb [12], this check yields a multiplicative factor of

TABLE I: Mean expected numbers of events in the control region ($m_{vis} < 120$ GeV/ c^2), compared with the numbers observed. The uncertainties listed include both statistical and systematic effects.

source	$e\tau_h$	$\mu\tau_h$	$\tau_h\tau_h$	total
$Z/\gamma^* \rightarrow e^+e^-$	0.1±0.1	-	-	0.1±0.1
$Z/\gamma^* \rightarrow \mu^+\mu^-$	-	0.5±0.3	-	0.5±0.3
$Z/\gamma^* \rightarrow \tau^+\tau^-$	45±7	38±6	4.2±0.8	88±12
jet $\rightarrow \tau_h$	4±1	4±1	3.2±0.6	11±2
total expected	49±7	43±6	7.4±1.0	99±13
observed	46	36	8	90

TABLE II: Mean expected numbers of events in the signal region ($m_{vis} > 120$ GeV/ c^2), compared with the numbers observed. (The numbers shown are rounded after adding.) The uncertainties listed include both statistical and systematic effects.

source	$e\tau_h$	$\mu\tau_h$	$\tau_h\tau_h$	total
$Z/\gamma^* \rightarrow e^+e^-$	0.2±0.1	-	-	0.2±0.1
$Z/\gamma^* \rightarrow \mu^+\mu^-$	-	0.5±0.3	-	0.5±0.3
$Z/\gamma^* \rightarrow \tau^+\tau^-$	0.6±0.1	0.5±0.1	0.4±0.1	1.4±0.3
jet $\rightarrow \tau_h$	0.3±0.1	0.2±0.1	0.3±0.1	0.8±0.2
total expected	1.0±0.2	1.2±0.3	0.6±0.1	2.8±0.5
observed	4	0	0	4

0.97 ± 0.10 , which is incorporated into the acceptance calculation in the simulation. The 10% uncertainty in this factor, which affects each identified τ_h in the selected sample, includes the trigger efficiency uncertainty.

The uncertainties in the e and μ identification and trigger efficiency, of 4% for e and 5.5% for μ , come from studies described elsewhere [5].

The jet $\rightarrow \tau_h$ fake background estimate has a 20% uncertainty reflecting the variation in the fake rate among the different trigger samples.

A 6% uncertainty due to imperfect modeling of the \cancel{E}_T comes from studies of transverse energy balancing in events with high energy jets recoiling against high energy photons.

Imperfect knowledge of the PDF’s leads to an 8% uncertainty in the DY and any new physics signal acceptances. The uncertainty is estimated from the variation of the acceptance using different PDF sets.

Table I summarizes the expected numbers of events by source for each channel, and shows the observed number of events in each search channel, for the control region dominated by Z boson decay ($m_{vis} < 120$ GeV/ c^2). The observed number is in good agreement with that expected. This gives confidence that the estimated efficiencies and background rates are well understood, and we proceed to examine the signal region.

Table II shows, for each search channel, the numbers of events expected and the uncertainty for each background source in the signal region ($m_{vis} > 120$ GeV/ c^2). We observe four $e\tau_h$ events, and no $\mu\tau_h$ or $\tau_h\tau_h$ events. Given the uncertainties shown in the table, the observed num-

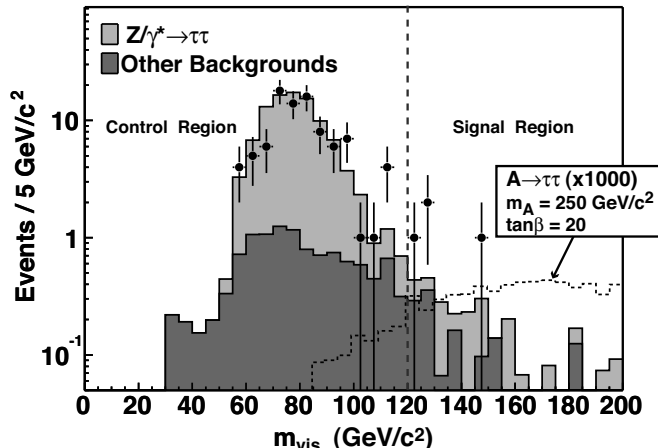


FIG. 2: Distribution of visible mass (m_{vis}) for data (points) and predicted backgrounds (shaded histograms) in the signal and control regions. The dashed histogram shows the distribution expected for a pseudoscalar Higgs A , with $m_A = 250$ GeV/c^2 and $\tan \beta = 20$, with the normalization increased by 1000. There are no observed events with $m_{vis} > 200$ GeV/c^2 .

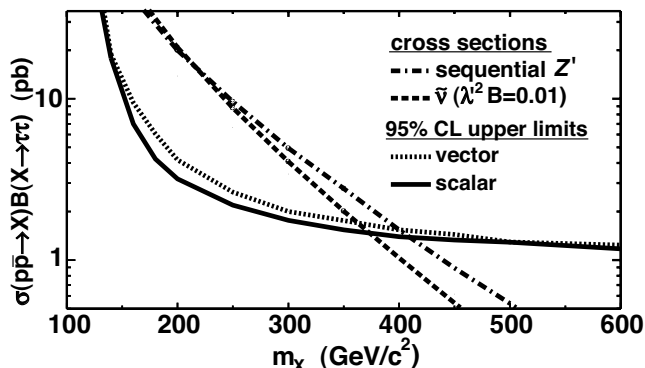


FIG. 3: Upper limits at 95% CL on the production cross section times branching ratio to tau pairs of scalar and vector particles, as a function of particle mass. The figure also shows the cross section times tau pair branching ratio for scalar neutrinos and sequential Z' bosons.

ber of events is in good agreement with that expected.

Figure 2 shows the distribution of visible mass in the signal and control regions, for the observed events and the predicted background. The distribution of the masses of the four events in the signal region is consistent with that expected from background.

Since we observe no significant excess rate of high-mass tau pair production, we determine upper bounds on the production cross section times branching ratio to

tau pairs of hypothetical scalar and vector particles. As a general model for the acceptance for scalar particle production we use pseudoscalar Higgs boson (A) production, and for vector particle production we use a Z' boson. The acceptance for both increases from near zero at masses of 100 GeV/c^2 to about 4% at high masses (500 GeV/c^2 or more).

To determine the upper bounds on the cross section times branching ratio we form a likelihood from the joint Poisson probability of all search channel results, and use a Bayesian method to incorporate the effects of systematic uncertainties, which are represented by truncated gaussian prior probability densities, including correlations. The likelihood is converted to a posterior probability density in the signal cross section using Bayes Theorem, assuming a prior in the signal rate which is uniform up to some high cutoff. The 95% CL upper limit comes from the integral of the posterior density.

Figure 3 shows the 95% CL upper bound on the cross section times branching ratio to tau pairs for scalar and vector particle production. Table III shows the upper limits on the production rate of scalar and vector particles as a function of mass. As an example of the sensitivity, these results would rule out a Z' with Standard Model couplings having a mass less than 399 GeV/c^2 , as indicated by the curve of cross section times branching ratio in the figure. The figure also shows the case of R-parity-violating scalar neutrino production and decay to tau pairs; this analysis, as an example, excludes a 377 GeV/c^2 scalar neutrino having coupling λ' to $d\bar{d}$ and branching ratio B to tau pairs such that $\lambda'^2 B = 0.01$. In general the limits are readily interpreted within the context of new physics models in which new scalar or vector particles decay to tau pairs.

We thank the Fermilab staff and the technical staffs of the participating institutions for their vital contributions. This work was supported by the U.S. Department of Energy and National Science Foundation; the Italian Istituto Nazionale di Fisica Nucleare; the Ministry of Education, Culture, Sports, Science and Technology of Japan; the Natural Sciences and Engineering Research Council of Canada; the National Science Council of the Republic of China; the Swiss National Science Foundation; the A.P. Sloan Foundation; the Bundesministerium für Bildung und Forschung, Germany; the Korean Science and Engineering Foundation and the Korean Research Foundation; the Particle Physics and Astronomy Research Council and the Royal Society, UK; the Russian Foundation for Basic Research; the Comisión Interministerial de Ciencia y Tecnología, Spain; in part by the European Community's Human Potential Programme; and the Academy of Finland.

[1] W. Hollik, Z. Phys. C37, 569 (1988); W. Hollik, Z. Phys.

C32, 291 (1986).

TABLE III: The 95% CL upper limits on scalar and vector particle production and decay to tau pairs.

mass (GeV/c^2)	120	140	160	180	200	250	300	350	400	450	500	600
scalar limit (pb)	87.3	17.9	7.00	4.23	3.19	2.19	1.76	1.54	1.40	1.33	1.29	1.17
vector limit (pb)	122	18.9	9.45	6.07	4.19	2.64	2.00	1.76	1.54	1.44	1.30	1.24

- [2] J.E. Gunion and H.E. Haber, Nucl. Phys. B272, 1 (1986); J.E. Gunion and H.E. Haber, Nucl. Phys. B278, 449 (1986).
- [3] D. Choudhury, S. Majhi, and V. Ravindran, Nucl. Phys. B660, 343 (2003); J. Kalinowski *et al.*, Phys. Lett. B414, 297 (1997).
- [4] M. Carena *et al.*, Phys. Rev. D70, 093009 (2004).
- [5] Z. Wan, "Search for High-Mass Tau Pairs in 1.96-TeV $p\bar{p}$ Collisions," thesis, unpublished, Rutgers University, 2005 (FERMILAB-THESIS-2005-13).
- [6] A dedicated Run I search is described in A. Connolly, "A Search for Supersymmetric Higgs Bosons in the Ditau Decay Mode in Proton-Antiproton Collisions at 1.8 TeV," thesis, unpublished, University of California, Berkeley, 2003 (FERMILAB-THESIS-2003-45).
- [7] D. Acosta *et al.*, Phys. Rev. D71, 032001 (2005).
- [8] We define the pseudorapidity η of a particle three-momentum as $\eta \equiv -\ln(\tan \frac{\theta}{2})$, where θ is the polar angle of the momentum to the beam direction.
- [9] S. Klimenko, J. Konigsberg, and T.M. Liss, FERMILAB-FN-0741 (2003).
- [10] S. Holm *et al.*, Trans. Nucl. Sci. 47, 895 (2000).
- [11] A. Anastassov *et al.*, Nucl. Instrum. and Methods, A518, 609 (2004).
- [12] D. Acosta *et al.*, Phys. Rev. Lett. 94, 091803 (2005).
- [13] T. Sjostrand *et al.*, Computer Phys. Commun. 135, 238 (2001), and references therein.
- [14] H. Lai *et al.*, Eur. Phys. J. C12, 375 (2000).
- [15] Z. Was *et al.*, Nucl. Phys. Proc. Suppl. 98, 96 (2001).